

Article

Giovanni Santi's Late 15th-Century Paintings: Microscopic, Spectroscopic and Chromatographic Investigations on Pigments, Powdered Glass and Binding Media

Maria Letizia Amadori ^{1,*}, Gianluca Poldi ², Mara Camaiti ³, Fabio Frezzato ⁴, Antonella Casoli ⁵,
Giulia Germinario ⁶, Elena Monni ⁴, Cecilia Pedulli ³ and Valeria Mengacci ¹

¹ Department of Pure and Applied Sciences, University of Urbino, P.za Rinascimento 6, 61029 Urbino, Italy; valeria.mengacci@uniurb.it

² Independent Researcher, Via del Pino 30, 20054 Milan, Italy; g.poldi@gmail.com

³ Institute of Geosciences and Earth Resources, National Research Council, Via G. La Pira n. 4, 50121 Florence, Italy; mara-camaiti@igg.cnr.it (M.C.); ceci.pedu@libero.it (C.P.)

⁴ Centro Ricerche sul Dipinto, C.S.G. Palladio—Lifeanalytics, Strada Saviabona 278/1, 36100 Vicenza, Italy; elena.monni@leanalytics.it (F.F.); elena.monni@lifeanalytics.it (E.M.)

⁵ Department of Chemistry, Life Sciences and Environmental Sustainability, University of Parma, Parco Area delle Scienze 17/a, 43124 Parma, Italy; antonella.casoli@unipr.it

⁶ Institute of Heritage Science-National Research Council (ISPC-CNR), Via per Monteroni, 73100 Lecce, Italy; giulia.germinario@cnr.it

* Correspondence: maria.amadori@uniurb.it; Tel.: +39-339-633-8838

Featured Application: This research paper contributes to improving the central Italy Renaissance database on painting materials and techniques.

Abstract: After a huge non-invasive diagnostic campaign performed on the corpus of Giovanni Santi's artworks, three paintings were selected and investigated: the *Martyrdom of Saint Sebastian* panel, the *Visitation* altarpiece and the canvas with *Tobias and the Archangel Raphael* (c. 1487 and 1494). Micro-invasive investigations including optical microscopy, ESEM-EDX, micro-Raman spectroscopy, FTIR and FTIR-ATR spectroscopy and GC-MS were carried out on selected micro samples. The results of the integrated analyses confirmed the use of a Renaissance palette with oil and, only in a few cases, tempera techniques. Some significant peculiarities emerged in Santi's practice, as he used localized off-white priming and colorless powdered glass with a siccativ oil—in red, flesh, pinkish and green hues—confirming the influence of the Flemish painters in Urbino and, possibly, also in western central Italy. This innovative technical expedient compared to the traditional Italian painting technique was identified also in red and bluish samples collected from the *Communion of the Apostles* panel painted by Justus of Ghent around 1473–1474 for Urbino Corpus Domini Confraternity. The Flemish master was called to the court of Duke Federico to paint in oil and his presence at the 'Urbino workshop' probably contributed to the diffusion of this technique. Both in Giovanni Santi's paintings and the *Communion of the Apostles*, the glass particles are related to a soda-lime glass typical of the Italian area, widely detected in Italian paintings from the late 15th and 16th centuries.

Keywords: spectroscopy; chromatography; painting materials; powdered glass; binder; Renaissance paintings



Citation: Amadori, M.L.; Poldi, G.; Camaiti, M.; Frezzato, F.; Casoli, A.; Germinario, G.; Monni, E.; Pedulli, C.; Mengacci, V. Giovanni Santi's Late 15th-Century Paintings: Microscopic, Spectroscopic and Chromatographic Investigations on Pigments, Powdered Glass and Binding Media. *Appl. Sci.* **2023**, *13*, 9739. <https://doi.org/10.3390/app13179739>

Academic Editor: Giuseppe Lazzara

Received: 21 July 2023

Revised: 17 August 2023

Accepted: 24 August 2023

Published: 28 August 2023



Copyright: © 2023 by the authors. Licensee MDPI, Basel, Switzerland. This article is an open access article distributed under the terms and conditions of the Creative Commons Attribution (CC BY) license (<https://creativecommons.org/licenses/by/4.0/>).

1. Introduction

This research on Giovanni Santi's paintings is part of an integrated multi-analytical campaign—based on the use of both non-invasive and micro-invasive techniques—aimed at investigating painting materials and practices during the Renaissance in western central Italy and particularly in Urbino, one of the most important art centers of that area [1].

This paper focuses on Santi's pictorial technique by examining two panel paintings, the *Martyrdom of Saint Sebastian* (1487–1488) (Figure S1a) and the *Visitation* (1488–1490) (Figure 1a), and a canvas painting, *Tobias and the Archangel Raphael* (1490–1494) (Figure 1b), unanimously attributed to Giovanni Santi and dating back between the late 1480s and the early 1490s [2–4].



Figure 1. Sampling areas in (a) *Visitation* altarpiece (c.1488–1490) and (b) *Tobias and the Archangel Raphael* canvas (c.1490–1494).

The *Martyrdom of Saint Sebastian* panel was executed for the confraternity of Saint Bartholomew in Urbino and placed in the oratory next to the homonymous church [4]. Its conservation history is troubled; in 1695, the painting suffered extensive damage caused by water infiltration. In 1750, it was subjected to a criticized restoration intervention that further damaged the painting. Restorations and repainting are documented in 1820 and 1900. The last significant intervention before 1971 was only focused on consolidating the surviving original pictorial film, integrating the large gaps in a neutral tone [5]. The *Visitation* altarpiece was commissioned for the church of Santa Maria Nuova in the Franciscan monastery in Fano. Its original location in the church is unknown but since the 18th century, it was moved to different sites in the Church. *Tobias and the Archangel Raphael* canvas, together with *Saint Roch*, was first documented in 1777 in the chapel of Saint Sebastian in San Francesco church of Urbino [2].

Based on the results of the non-invasive diagnostic campaign [6], Giovanni Santi's paintings were submitted to careful sampling (Table S1), and micro-invasive techniques (polarized light microscopy, ESEM-EDX, micro-Raman, FTIR, FTIR with micro-ATR spectroscopy and GC-MS) were used to investigate painting materials and binders. The research aimed specifically to identify the presence of colorless powdered glass as hypothesized by the previous non-invasive investigation results.

Recent and in-depth studies reassess the figure of Giovanni Santi (1439 ab.–1494), both as a non-secondary actor in the lively cultural life of the court of Urbino [3,7] and as a painter probably open to innovations and influences of Flemish techniques [1,2].

At the end of the 15th century, many Italian artists achieved a gradual transition from the tempera technique—based above all on the use of egg yolk as a binder—to the oil technique. The contact with the Flemish painter Justus of Ghent, working in Urbino

from the 1470s [8], probably allowed Santi to experiment with the still innovative—at that time—oil technique.

A deep comparison was carried out with the main technical features that emerged from the study of the *Communion of the Apostles* painted by Justus of Ghent in Urbino and currently in the Ducal Palace in Urbino (Figure S1b, Table S1) [9–11]. The oil panel was initially commissioned to Paolo Uccello—who completed only the predella in the last years of his life, 1467–1468—then to Piero della Francesca who came to Urbino in 1469 as a guest of Giovanni Santi but renounced for reasons still unknown [7]. Almost four years later, the panel was assigned to Justus of Ghent, who worked on it around 1473–1474 [12].

2. Oil Painting and Italy

The awareness of different technical characteristics between the world of Italian painting and that of the northern Alps artists already emerges from a short passage in the *Book of the Art (Libro dell'arte)*, a treatise written at the end of the 14th century by Cennino Cennini, a painter active for a certain period in Padua, but proudly and openly rooted in the Tuscan and Giotto tradition: “Before going any further, I want to teach you how to work with oil on wall or panel, as the Germans often do” [13]. Indeed, in very few points of the treatise, Cennini goes into detail about the use of oil, apart from a generic invitation to grind the colors with oil or to use them according to personal taste [13]. Among the pigments miscible with oil, he mentions verdigris, red lakes and, only in two cases, ultramarine blue and black ([13], in part, chapter CLXXII). However, those indications should not be considered accidental, but probably deriving from the artist’s mastery of the oil technique.

In Cennini’s passages, however, there are no signs of fascination with Nordic painting whose exponents were certainly present in Padua, an important hub in the connection between the Peninsula and the northern area of the Alps. Instead, it took almost fifty years to spread the interest in Nordic painting, and especially Flemish, from the Italian courts and through their artists. From Naples to Milan, from Ferrara to Urbino, the fame of the most important Flemish painters became widespread between the 1440s and 1470s. The fame of Jan Van Eyck and Rogier Van der Weyden, the latter visited Italy in 1450, is testified by historical sources and was cited by the humanist Bartolomeo Facio in his *De viris illustribus* dedicated to the king of Naples Alfonso d’Aragona, while Giovanni Santi himself praised the two Flemish artists in his *Cronaca Rimata* [14]. The admiration and curiosity for the technical solutions adopted by the Flemings can also be deduced from the important experiments conducted by Piero della Francesca on some of his masterpieces, as well as other Italian artists [15–17]. Zanetto Bugatto’s long educational trip from Milan to the workshop of Van der Weyden between 1460 and 1463 is particularly notable [18].

The substantial extraneousness to the systematic use of the oil technique compared to tempera emerges in the Architectural Treatise by Antonio Averlino known as Filarete, composed precisely in Milan between 1451 and 1464: “And so, if you have to paint in tempera and also in oil, you can put all these colours, but this is another practice and another way, which is beautiful, for those who know how to do it”, then citing Jan Van Eyck and Rogier Van der Weyden, “who have excellent use of these oil colours” [19]. Filarete goes into a little more detail in a further part of his treatise in which he writes about linseed oil and mentions the methods of application [19]. The situation would change only after the mid-1480s when the mastery of the use of oil became part of the technical background of many Italian painters [20,21].

3. Materials and Methods

3.1. Sampling

A set of twenty-five representative micro samples were collected from the *Martyrdom of Saint Sebastian* panel (GSM), *Visitation* altarpieces (SF) and *Tobias and the Archangel Raphael* canvas (GSS) made by Giovanni Santi (Table S1, Figure S1a and Figure 1a,b). The paintings were sampled before the restoration interventions related to Santi’s exhibition held in Urbino between 2018 and 2019 (3). Four samples were collected from repainted areas of

both the *Martyrdom of Saint Sebastian* panel and *Tobias and the Archangel Raphael* canvas due to the difficulty in removing them during the last restoration intervention. The sampling was carefully carried out by detaching a micro fragment (1–2 mm), on the basis of preliminary non-invasive investigations [6], from both the painting layer and the wood or canvas supports.

Two micro samples collected from the *Communion of the Apostles* panel (CA) (Figure S1b) [10] painted by Justus of Ghent, were also considered.

The list of the samples and the performed analyses are given in Table S1.

3.2. Polarized Light Microscopy (PLM)

The wooden sample (GSM9) collected from the *Martyrdom of Saint Sebastian* panel (Table S1) was prepared following the standard procedure [22,23]. A thin section was investigated in transmission light to identify the characteristic microscopic anatomical features. The fiber samples (SF9, GSS5) were observed to reflected light (Table S1).

Some painting samples were embedded in epoxy resin support (SeriFix resin, Struers) and then carefully polished after curing the resin with progressively finer silicon carbide cards. Darkfield and bright-field observations on cross-sections (Table S1) were performed using an OLYMPUS BX51 polarized light microscope, equipped with fixed oculars of 10× and objectives with different magnifications (5, 10, 20, 50 and 100×), and directly connected to Olympus SC50 camera and to Stream Basic software for images acquisition. A mercury-vapor lamp, Olympus U-LH 100HG APO 19V 100W, was used for UV light observations.

3.3. Environmental Scanning Electron Microscopy Coupled with Energy Dispersive X-ray Detector (ESEM/EDX)

Morphological observations and chemical microanalyses were carried out on cross-sections using an environmental scanning electron microscope (Philips Quanta FEI 200) equipped with an energy-dispersive X-ray spectrometer (EDX) by Link Analytical Oxford (Link, UK), model 6103. Cross-sections were investigated by applying them on aluminum stubs with Ag-conductive glue. The morphology of fiber samples (SF9, GSS5) was observed too. The analyses were performed at acceleration voltage from 15 kV to 20 kV with a variable working distance (from 7.3 to 11.4 mm), 40 μA filament current, 100 s acquisition time.

For the semi-quantitative analyses of the glass particles, only the larger ones were selected and analyzed. In order to level all data, some elements, such as carbon, chloride, mercury, sulfur and copper were subtracted, and values were normalized.

3.4. Fourier Transform Infrared Spectroscopy (FTIR and Micro-FTIR with ATR)

The investigation of the binder was carried out in two steps and with two different approaches: the first part of the analytical procedure was carried out by FTIR on sample fragments (Table S1). The second stage was focused on obtaining as much information as possible from each layer, and for that reason, the analysis was carried out by micro-FTIR (FTIR-ATR) directly on microstratigraphic sections (Table S1).

The FTIR spectra were recorded by a Spectrum 1000 Perkin-Elmer spectrometer, equipped with the software “Spectrum” for data processing. The micro-samples, selected under a stereomicroscope (Nikon mod. SMZ745T), were analyzed as such without further manipulation in transmission mode using a diamond anvil cell (Specac, Slough England). The working spectral range was from 4000 to 400 cm⁻¹, with a resolution of 2 cm⁻¹ and 64 scans.

Micro-FTIR analysis was carried out on the cross-sections of samples and the spectra were taken from each layer in attenuated total reflectance mode (ATR) or in specular reflection mode employing a ThermoNicolet “Continuum” Nexus line micro spectrophotometer, equipped with an MCT detector. In the ATR mode, a micro-slide-on ATR silicon crystal directly connected to the objective was used. The contact area of the ATR silicon crystal is circular and approximately 100 μm in diameter. However, the area of the layer actually

measured is given by the contact area divided by the refractive index of the crystal (refractive index of silicon crystal is 3.4) and, hence, is about 30 μm in this case; it can be further reduced to near the diffraction limit by the use of an aperture. The measured areas depend also on the contact pressure. Infrared spectra were recorded in the 4000–650 cm^{-1} ranges with resolution of 4 cm^{-1} and 120 scans. All spectra collected on the micro-samples are given in transmittance units after baseline correction.

3.5. Micro-Raman Spectroscopy

Micro-Raman spectra were recorded with a Labram instrument from the Jobin Yvon-Horiba, equipped with a red 633 nm laser, a Peltier-cooled ($-70\text{ }^{\circ}\text{C}$) CCD detector with 1024×256 pixels; a spectral resolution of 1 cm^{-1} , and a spatial resolution of 1 μm . According to the intrinsic intensity of the spectrum recorded, the scanning time varied from 5 to 20 s and the number of scans from 5 to 20 with the laser power (5 mW) attenuated to about 1/10. Olympus long-distance objectives with 50 and 100 enlargements were used. Raman analyses were performed only on some of the cross-sections.

3.6. Gas Chromatography-Mass Spectrometry (GC-MS)

A Focus GC (Thermo Scientific) coupled to DSQ II (Thermo Scientific) with a single quadrupole and split-splitless injector was used. The carrier gas was used in the constant flow mode (He, purity 99.995%) at 20 mL/min. The injector was kept at 280 $^{\circ}\text{C}$. Separation of analytes was performed by means of a fused-silica capillary column (RXI-5, Restek) with a 0.25 μm (30 m \times 0.25 mm \times 0.25 μm) methyl-silicone (5% phenyl) film. MS conditions were as follows: interface temperature at 280 $^{\circ}\text{C}$; ion source temperature at 230 $^{\circ}\text{C}$. The mass spectrometer was operated in the EI positive mode (70 eV). The mass spectra were collected with a 41–500 m/z fragmentation rate.

The analysis was carried out using a sample quantity of less than 1 mg (Table S1). The considered internal standards were: tetracosane (50 μL of a 0.1 mg/mL solution *w/v*) for the fatty acids analysis; norleucine (50 μL of a 0.1 mg/mL solution *w/v*) for the amino acids analysis.

For the fatty acid extraction, the sample was treated with 4N-HCl in methanol (1 mL) and n-hexane (1 mL) for 2 h at 50 $^{\circ}\text{C}$. The n-hexane phase containing fatty acid methyl-esters was used for GC-MS analysis (1 μL). Separation of the methyl ester of fatty acids was achieved using the following temperature program: isothermal conditions at 60 $^{\circ}\text{C}$ for 2 min, with 20 $^{\circ}\text{C}/\text{min}$ heating up to 220 $^{\circ}\text{C}$ and isothermal conditions at 220 $^{\circ}\text{C}$ for 8 min, lasting up to 280 $^{\circ}\text{C}$ with an increment of 20 $^{\circ}\text{C}/\text{min}$ and 4 min at 280 $^{\circ}\text{C}$. The mass spectra were collected with a 40–400 m/z fragmentation rate. After the previous phase, the extraction of amino acids was carried out: after dry evaporation of the residual methanol phase, the residues were dissolved using 6N hydrochloric acid (2 mL) and hydrolyzed in a screw-capped container for six hours at 90 $^{\circ}\text{C}$ in an oil bath, under a nitrogen atmosphere.

For the amino acids' extraction, after evaporation, the methanol phase to dryness, the residues were dissolved in 6N hydrochloric acid (2 mL) and hydrolyzed in a screw-capped container for six hours at 90 $^{\circ}\text{C}$ in an oil bath under a nitrogen atmosphere. After evaporation to dryness, the hydrolyzed residues were esterified using 0.4 mL of 2N HCl in propane-2-ol at 90 $^{\circ}\text{C}$ for one hour. After cooling, the solvent was evaporated under vacuum and the residue was dissolved in 0.3 mL of dichloromethane and derivatized with 0.2 mL of trifluoroacetic anhydride at 60 $^{\circ}\text{C}$ for 30 min. After evaporation to dryness, the residue of the paint sample was dissolved in 0.3 mL of dichloromethane, and then the solution was used for GC-MS analysis (1 μL). The separation of N-trifluoroacetyl-O-2-propyl esters amino acids derivatives was achieved using the following temperature program: isothermal conditions at 60 $^{\circ}\text{C}$ for 3 min, with 20 $^{\circ}\text{C}/\text{min}$ heating up to 280 $^{\circ}\text{C}$ and isothermal conditions at 280 $^{\circ}\text{C}$ for 12 min.

The basic methodology relied on the identification of fatty acids and amino acids in the same samples. Two chromatograms were collected for each sample: the first for fatty acid derivatives and the second for amino acid derivatives [24].

To identify the proteinaceous binders, the percentage content of amino acids in each sample was related to those from a dataset of 43 reference samples of egg (whole, egg white, egg yolk), skimmed milk, animal glue, and the mixtures of them [25,26]. Principal component analysis (PCA) was carried out on the relative percentage of eight amino acids (aspartic acid, glutamic acid, proline, hydroxyproline, phenylalanine, alanine, glycine and leucine) using the correlation matrix of the values [27].

4. Results

The integrated analyses allowed us to identify the painting materials and the binding media used by Giovanni Santi in the selected paintings made between c.1480 and 1494: the *Martyrdom of Saint Sebastian*, the *Visitation* panels and the *Tobias and the Archangel Raphael* canvas. A comparison with the *Communion of the Apostles* [9–11] painted by Justus of Ghent in c.1473–1474, was also performed looking for the presence of colorless powdered glass.

All the data obtained related to supports, ground layers, underdrawings, pigments (organized by color) and painting techniques are reported and discussed below with the associated tables and related images. More information is available in the supporting materials (Figures S1–S10).

4.1. Supports

As evidenced by PLM morphological investigations (sample GSM9: Figure S2a, Table S1), the wood species used both in the *Martyrdom of Saint Sebastian* panel and the *Visitation* altarpiece belong to the genus *Populus* sp. of the Salicaceae family.

A protective layer was applied to the back of both paintings. PLM observations, in Vis and UV light (sample SF8: Figure S2b, Table S1), confirmed the presence of a brownish film-forming substance (probably glue) on the wooden support followed by a ground layer (200 μm thickness) and a reddish layer (50 μm). ESEM-EDX analysis of the backside sample detected Ca and S, related to calcium sulphate, in the ground layer, while Pb is the main element in the red lead-based reddish layer.

According to the nodes' structures, linen canvas strips (sample SF9: Figure S2c, Table S1) were identified on the front side (recto) of the panel, along the board joints, on metallic elements and in proximity of butterfly keys to reduce stresses and damages to the painting film of the *Visitation* altarpiece.

ESEM-BSE observations of fibers collected from the herringbone canvas support of *Tobias and the Archangel Raphael* (sample GSS5: Figure S2d, Table S1) [2] revealed the typical linen morphology with node structure [28].

4.2. Preparatory and Priming Layers

PLM observations and ESEM-EDX carried out on the *Martyrdom of Saint Sebastian* panel and the *Visitation* altarpiece (Tables S1–S3) showed the presence of one or two ground layers. The inner one contains coarse grain size gypsum particles (derived from the so-called “gesso grosso” or burnt gypsum [29], along with a few large quartz crystals and silicates, followed by a gypsum layer made of fine particles (obtained from “gesso sottile” or slaked burnt gypsum with an excess of water). Impurities of Si, Mg, Fe, Al and K are related to silicates (sample GSM1: Figure S3a–c; samples GSM5, GSM7: Table S2). The maximum thickness of the ground layer is around 450–480 μm (Tables S2 and S3).

The FTIR spectrum of almost all the ground samples shows the characteristic signals of both calcium sulphate dihydrate (gypsum, $\text{CaSO}_4 \cdot 2\text{H}_2\text{O}$) and anhydrous (anhydrite, CaSO_4) (Table S2). Indeed, structured bands are evident in the ranges 1160–1130 cm^{-1} , corresponding to the asymmetric stretching of SO_4^{2-} ; and 590–680 cm^{-1} ($\nu_4(\text{SO}_4^{2-})$ mode). In particular, the peaks at 1138, 1117, 670 and 602 cm^{-1} of respective samples GSM1, GSM4, GSS1a and GSM6 in Figure 2a are assigned to gypsum, whereas those at 1150, 1112, 675, 611 and 594 are, respectively, assigned to anhydrite. The two bands between 3552 and 3406 cm^{-1} and two peaks at 1685 and 1622 cm^{-1} could be respectively assigned to the -OH stretching and bending of the water molecules of gypsum [30] (Figure 2a).

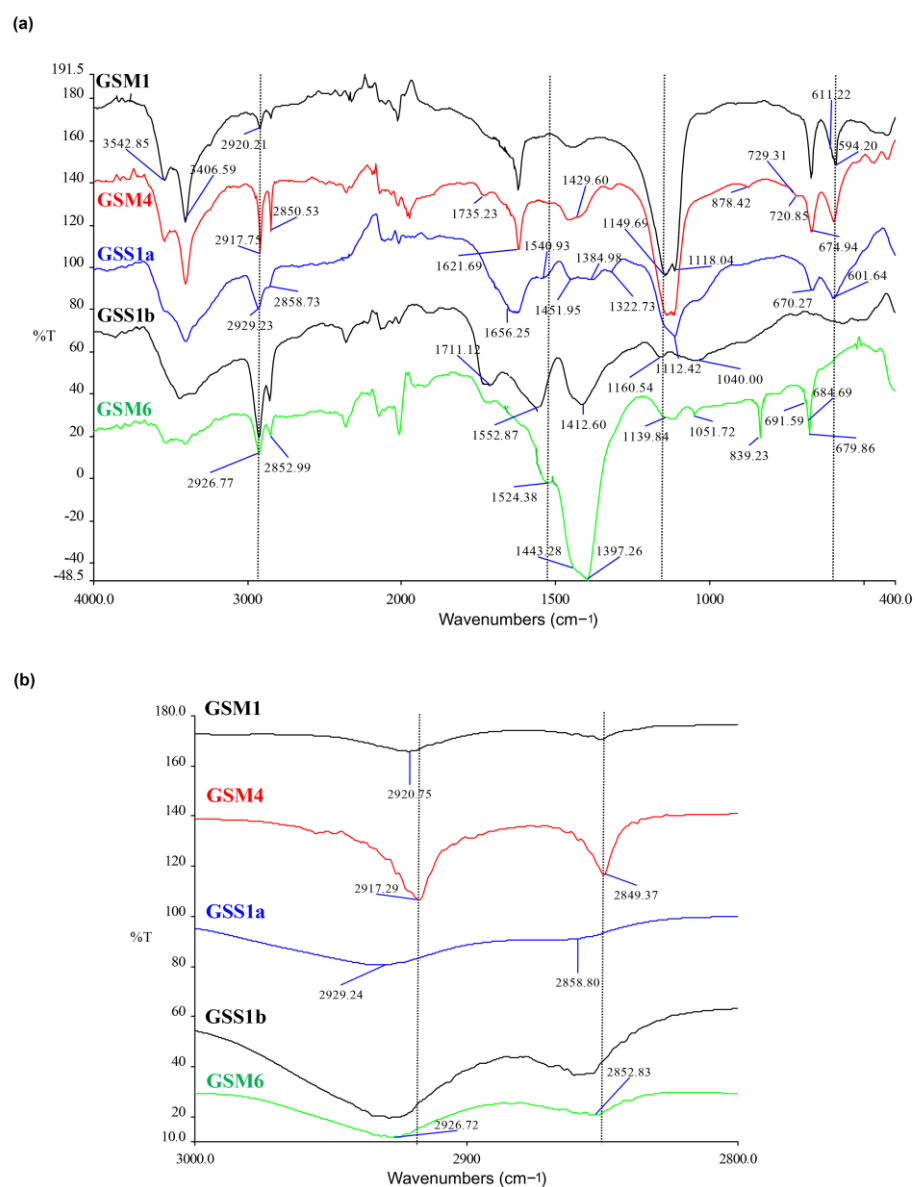


Figure 2. *Martyrdom of Saint Sebastian* panel and *Tobias and the Archangel Raphael* canvas: (a) FTIR spectra of the ground layer of samples GSM1, GSM4, GSM6, GSS1a (light brown ground), GSS1b (dark brown ground); (b) Detail of the spectra in the range 3000–2800 cm⁻¹. The dotted lines are meant to show the shift of the signals in the region of interest for different samples.

The presence of anhydrite is consistent with the use of *gesso grosso* in the inner ground layers. Regarding the organic material (binding materials), the FTIR spectra of all ground samples show a complex pattern in which several compounds can be present at the same time. Overall, wax is present in many samples, as well as esters of carboxylic acids and carboxylates, calcium oxalates and proteinaceous materials (Table S2). Only in one sample, GSM6 corresponding to the priming layer, cerussite (CO₃²⁻ asym stretch at 1438 cm⁻¹ and 1405 cm⁻¹, CO₃²⁻ sym stretch at 1052 cm⁻¹, and in plane CO₃²⁻ bending at 680 cm⁻¹) [31] and lead white (OH stretch at 3538 cm⁻¹, CO₃²⁻ asym stretch at 1397 cm⁻¹ CO₃²⁻ sym stretch at 1046 cm⁻¹, and out-of-plane and in plane CO₃²⁻ bending at 840 and 683 cm⁻¹, respectively) [32] were detected together with esters of carboxylic acids, lead carboxylates and traces of gypsum (Figure 2a). Esters of carboxylic acids (oils) and lead carboxylates can be inferred from the signals at 2926–2929 and 2850–2 cm⁻¹ (CH₂ stretch), 1728 cm⁻¹ (C=O stretch of esters of carboxylic acids) [33], and 1524 cm⁻¹ (asym stretch of carboxylates) [34]. However, due to the non-homogeneity of the substrate and the selectivity of the sampling,

the substances identified in each spectrum can be slightly different, both in composition and concentration. According to the spectrum, GSM1 consists of a mixture of a waxy material mixed with low amounts of lipidic compounds and carboxylates, calcium oxalates (diagnostic signal of the CO sym stretch in oxalate anion at 1318–1325 cm^{-1} [35] and proteinaceous material (amide I at 1650 cm^{-1} and amide II at about 1543 cm^{-1}) [36]. In particular, the signal at 2920 cm^{-1} is assigned to CH₂ stretch due to the combination of CH₂ stretch in waxy material (2918 cm^{-1}) and CH₂ stretch in lipidic compounds (2926–2929 cm^{-1}), while the weak signals at 1318 cm^{-1} , 1650 cm^{-1} and 1545 cm^{-1} are better evidenced in the unsmoothed spectra. On the other hand, the spectrum of GSM4 shows peaks assigned to waxes (CH₂ stretch at 2918 and 2850 cm^{-1} , C=O stretch at 1735 cm^{-1} , CH₂ scissoring at 1470 and 1460 cm^{-1} , CH₂ rocking vibration at 729 and 720 cm^{-1}) [37]. In contrast, the spectrum of GSM4 shows peaks assigned to waxes and small amounts of calcium oxalates. Instead, GSM6, as already reported, contains signals due to lipidic and carboxylate products. For the sake of clarity, it should be noted that the identification of oils and waxes in complex mixtures by FTIR is not easy due to both the low signal intensity (due to the low concentration of the organic materials) and the co-presence of peaks of other compounds in the spectrum. In this work, the range 3000–2800 cm^{-1} has been considered as a diagnostic region for the identification of oils and waxes. Indeed, oils and waxes have strong peaks in this region, contrary to the other compounds frequently found in paintings. A detail of the 3000–2800 cm^{-1} region for samples GSM1, GSM4, GSS1a, GSS1b and GSM6 is shown in Figure 2b.

According to stratigraphic investigations and FTIR, the ground layer of *Tobias and the Archangel Raphael* canvas is made of gypsum with quartz and aluminosilicates impurities and has a maximum thickness of 150 μm (Tables S1 and S4). The FTIR spectrum of GSS1a (light brown ground) shows signals assigned to gypsum, proteinaceous material, silicates, calcium oxalates and partially hydrolyzed esters of carboxylic acids and their carboxylates (Figure 2a). Meanwhile, the FTIR spectrum of GSS1b (dark brown ground) shows peaks due to partially hydrolyzed esters of carboxylic acids and their carboxylates, silicates, sulphates (e.g., magnesium or iron sulphate) and traces of oxalates.

PLM and ESEM-EDX observations of the flesh (sample SF1, Table S3) from the *Visitation* altarpiece detected a priming layer (5 μm) composed of lead white and Fe-based pigments [38]. Lead white, Fe-based pigments and a few orpiment particles were revealed in the off-white priming of the Virgin's blue mantle (sample SF6: Figure S4a–c, Table S3).

4.3. Underdrawing

Micro Raman analysis of the black particles related to the underdrawing of the *Visitation* altarpiece showed broad bands around 1587 and 1345 cm^{-1} , corresponding to G and D bands, respectively, due to the vibrational density of state which could be ascribed to carbon black pigment [39] (sample SF1: Figure S5, Table S3). The use of liquid carbon-based ink for the underdrawing was previously attested through the IR reflectography campaign [6].

4.4. Pigments and Dyes

4.4.1. Blue and Violet Hues

According to PLM and ESEM-EDX investigations, the pale blue mountain of the *Martyrdom of Saint Sebastian* panel consists of a thin painting layer (50 μm thick), mainly composed of lead white, large azurite particles with Ag impurities, calcium carbonate and silicates (sample GSM5: Figure S6a–c, Table S2).

FTIR and FTIR-ATR analysis carried out on the cross-sections of the blue samples (GSM5 and GSM10) confirmed the occurrence of azurite mixed with lead white in different proportions and with small additions of other pigments depending on the hues. In the acquired spectra of the blue grains of sample GSM5, the presence of azurite can be inferred by the characteristic bands at 3419 cm^{-1} (stretching of the O-H bond), and at 1513 and 1414 cm^{-1} due to the stretching ν_3 of the CO_3^{2-} ion. In addition, the bands at 956 cm^{-1} ascribed to the out-of-plane bending of the O-H bond, and at 836 cm^{-1} , due to the stretching

ν_2 of the CO_3^{2-} ion, were detected (Figure 3, Table S2) [40]. Bands and peaks indicative of the use of a lipoprotein binder (assigned to egg) were also observed (2924, 2854, 1735, 1648, 1538 cm^{-1}) (Figure 3). The relatively broad peak at 1708 cm^{-1} was ascribed to carboxylic acids derived from the hydrolysis of eggs' esters. Lead white, detected on the pictorial layer (a white matrix that includes blue crystals) by FTIR-ATR, was identified by IR spectral features associated with the CO_3^{2-} rocking deformations (683 and 692 cm^{-1}) and the symmetric CO_3^- stretching vibration at 1044 cm^{-1} . Additionally, the antisymmetric CO_3^- stretching vibration (1407 cm^{-1}) and the hydroxyl stretching vibration at 3535 cm^{-1} can be observed [32].

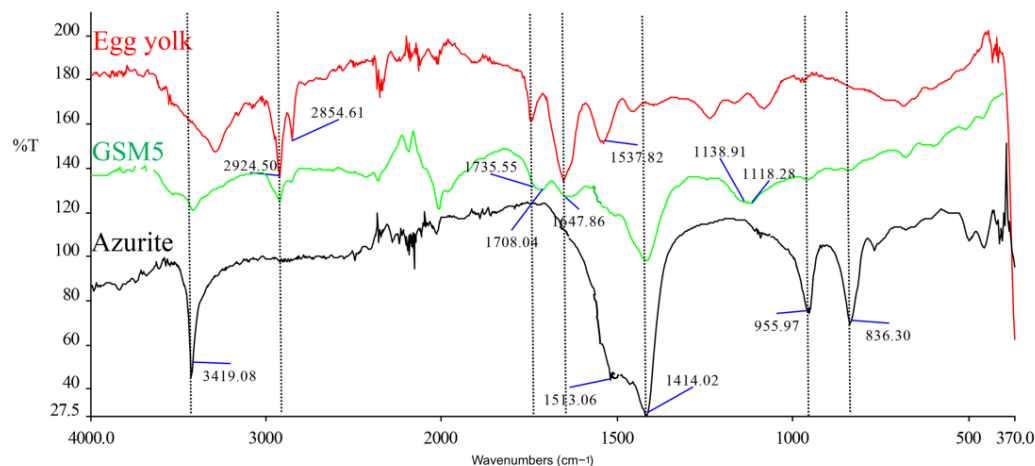


Figure 3. *Martyrdom of Saint Sebastian* panel: FTIR spectra of sample GSM5 (blue pictorial layer), egg yolk and azurite.

The presence of gypsum (peaks at 1118 and 1139 cm^{-1}) and quartz (peaks at 1080 and 460 cm^{-1}) was also detected [41,42].

The violet-blue hue of Saint Sebastian's loincloth (sample GSM7, Table S2) is composed of a thin layer ($50\text{ }\mu\text{m}$) of azurite, silicates lead white, bone black and red lake particles (Figure S6d,e). PLM and ESEM-EDX allowed to distinguish the red lake particles due to the high peak of Al [43] as confirmed by previous reflectance spectroscopy measurements carried out in that area [6]. FTIR analysis allowed the identification of azurite and egg as a binder.

In the *Visitation* altarpiece, the shadow of the Virgin's blue mantle consists of a layer ($90\text{ }\mu\text{m}$ thick) composed of finely grounded azurite, silica and rare hematite particles (sample SF6: Figure S4a, Table S3) [44]. Micro-FTIR analysis confirmed the use of azurite (Figure S6f).

Two painting layers were identified in the Archangel Raphael's violet robe (sample GSS4, Table S4): a first one ($10\text{ }\mu\text{m}$) composed of a red lake followed by a thicker layer ($40\text{ }\mu\text{m}$) mainly made of lead white, red lake particles and natural ultramarine. The red lake presence [43] was also confirmed by previous reflectance spectroscopy measurements [6]. FTIR-ATR analysis confirmed the presence of natural ultramarine (peak of Si, Al-O asym stretch at 979 cm^{-1}) [45,46], lead white, small amounts of esters of carboxylic acids, lead carboxylates (peak at 1526 cm^{-1}) and proteinaceous material (due to amide I at 1650 cm^{-1}). The presence of lead carboxylates with very small amounts of non-hydrolyzed esters suggests the use of oil as a binder; however, the occurrence of the proteinaceous material could be related to egg binder.

4.4.2. Green Hues

In the *Martyrdom of Saint Sebastian* panel, the vegetation in the background showed quite a complex stratigraphy. The underlayer ($44\text{ }\mu\text{m}$ thick) is composed of Cu-based pigments, lead white, rare particles of lead-tin yellow and dolomite. The superimposed

pictorial layer (50 μm), which appears more transparent under PLM, consists of a Cu-based matrix, lead-tin yellow and rare orpiment particles. The final layer (10 μm) contains lead white admixed with Cu-based pigments (sample GSM4: Figure S7a, Table S2). The infrared spectrum of the green pictorial layer of sample GSM4 is shown in Figure 4a.

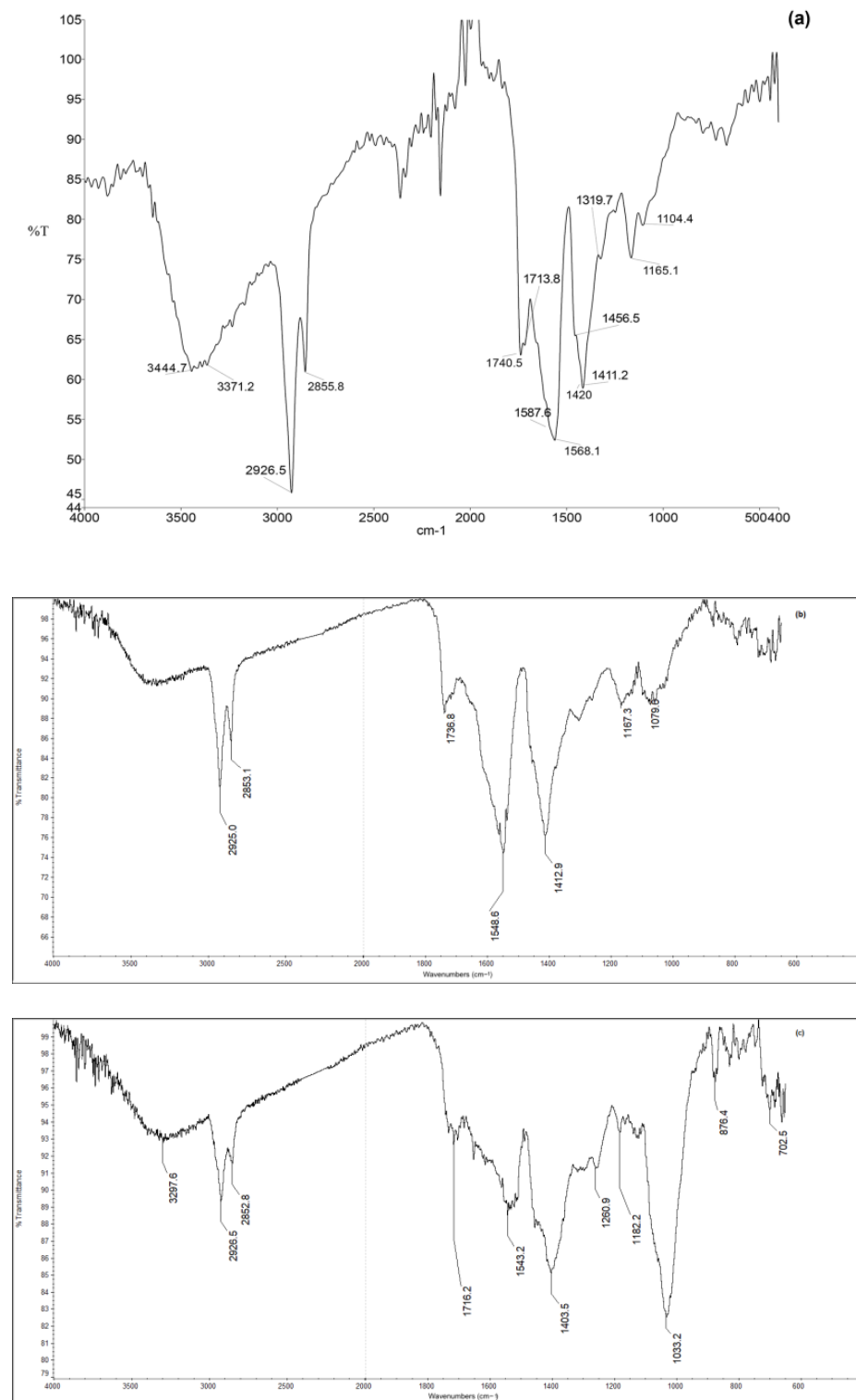


Figure 4. *Martyrdom of Saint Sebastian* panel and *Visitation* altarpiece: (a) FTIR spectrum of the green pictorial layer of sample GSM4; (b) FTIR-ATR spectrum of the green pictorial layer of sample SF5; (c) FTIR-ATR spectrum of the yellow pictorial layer of sample SF5.

The green color has been identified as verdigris basic (chemical formula $\text{Cu}(\text{CH}_3\text{COO})_2[\text{Cu}(\text{OH})_2]_3 \cdot 2\text{H}_2\text{O}$) for the characteristic peaks at 1568 and 1415 cm^{-1} (asym and sym stretch of copper carboxylate, respectively) and at 3371 cm^{-1} (OH stretch) [47,48]. The use of oil as a binding medium is supported by the peaks at 2926 , 2855 and 1740 cm^{-1} , as well as by the presence of other peaks due to CO stretch of carboxylic acids (1713 cm^{-1}), and COO^- stretch of copper carboxylates (1586 – 1587 cm^{-1} and 1417 – 1421 cm^{-1}), partially covered by the signals of copper acetate (verdigris basic) [34].

Cerussite and hydrocerussite were detected with Raman analysis in sample GSM4 for the main bands at 1053 and 1057 [49] along with lead-tin yellow type I (Figure S7b) 200 , 133 cm^{-1} [50].

In the green mantle of the noblewoman of the *Visitation* altarpiece (sample SF2, Table S3), the light green underlayer ($25\text{ }\mu\text{m}$) is composed of a Cu-based pigment, lead-tin yellow, lead white and silica particles. The two overlapped layers are made of verdigris basic and lead-tin yellow as confirmed by FTIR.

The stratigraphy of sample GSS1, related to the green hue of *Tobias'* robe (Table S4) showed a light green underpaint made up of two layers. The first one ($50\text{ }\mu\text{m}$) is composed of Cu-acetate (verdigris basic, as confirmed by FTIR) mixed with lead white, lead-tin yellow, a few scattered particles of orpiment and finely glass powdered particles (Table 1). The second ($60\text{ }\mu\text{m}$), slightly darker, is based on Cu-acetate-based pigment with rare lead-tin yellow and Fe-based particles. The subsequent glaze layer ($30\text{ }\mu\text{m}$) consists of verdigris basic and orpiment.

Table 1. Quantitative ESEM-EDX analysis of the powdered glass particles, normalized and expressed as weight % oxide. Glass particles were found in Giovanni Santi's paintings (*Visitation altarpiece*-SF, *Martyrdom of St. Sebastian* panel-GSM, *Tobias and the Archangel Raphael* canvas-GSS) and Justus of Ghent's painting panel (*Communion of Apostles*-CA).

Samples Code	Painting Layer Color	Layer	Maximum Glass Particles Size (~ μm)	Na ₂ O	MgO	Al ₂ O ₃	SiO ₂	K ₂ O	CaO	MnO	Fe ₂ O ₃	PbO
SF1	Flesh	2	20	6.71	3.17	1.9	62.88	1.69	10.86	0.72	0.92	11.15
SF3	Dark red	2	20	12.13	4.72	2.46	64.71	1.26	7.49	0.69	0.64	5.9
	Light red	1	30	13.81	4.71	1.22	65.75	1.47	8.76	0.4	0.37	10.33
SF4	Dark red	2	20	13.63	6.84	1.99	64.91	1.28	9.75	0.51	0.18	0.9
	Pinkish	1	30	9.52	2.02	0.18	57	5.05	18.59	0.32	0.63	6.69
GSS1	Green	1	45	16.57	4.76	2.07	59.32	2.52	12.34	0.41	0.6	1.87
GSS3	Red	1	30	15.95	7.16	1.38	63.86	1.19	9.23	0.23	0.15	0.84
GSM6	Red	3	30	7.29	3.15	5.07	61.77	2.11	8.94	0.81	0.61	10.27
			Average value	11.95	4.57	2.03	62.53	2.07	10.75	0.51	0.51	5.99
CA2	Red	2	20	7.98	4.03	5.53	64.16	3.59	10.28	1.58	0.75	2.1
CA7	Blue	2	20	2.89	1.23	2.77	22.97	1.76	6.53	0.6	0.47	9.08
			Average value	5.44	2.63	4.15	43.57	2.68	8.41	1.09	0.61	5.59

4.4.3. Yellow and Brown Hues

In the rocks of the *Martyrdom of Saint Sebastian* panel (sample GSM11, Table S2) PLM and ESEM/EDX analyses showed the presence of vermilion, lead white, Cu-based particles and ochre mixed together to achieve a reddish-brown hue.

The shadow of Saint Joseph's yellow mantle in the *Visitation* altarpiece (sample SF5, Table S3) revealed a complex layer structure: the greenish underlayer ($60\text{ }\mu\text{m}$) is made of verdigris basic, as confirmed by FTIR-ATR (Figure 4b), along with lead white and lead-tin yellow; in the second yellowish layer ($60\text{ }\mu\text{m}$), ochre was detected in addition to this mixture; the last overlapped painting layer ($8\text{ }\mu\text{m}$) appears rich in ochre particles. FTIR-ATR analysis confirmed the presence of lead white and also detected silicates (peak

at 1032 cm^{-1}) and lipidic compounds (mainly carboxylates, peak at 1542 cm^{-1} , and small amounts of carboxylic acids, peak at 1716 cm^{-1} , and esters) (Figure 4c).

The Archangel Raphael's cloak (sample GSS2, Table S4) consists of a first yellow opaque layer ($83\text{ }\mu\text{m}$) of lead-tin yellow with small amounts of hematite and Fe-based (earth) pigments, followed by a glaze layer composed of earth pigments and bone black.

4.4.4. Red Pinkish and Flesh Hues

PLM and ESEM-EDX investigations carried out on the red (sample GSM1) and pinkish (sample GSM2) hues of the *Martyrdom of Saint Sebastian* panel (Table S2) showed an underpaint layer composed of different amounts of vermilion, lead white and red lake particles. The overlapped glaze layer is composed of a red lake glaze with powdered glass particles found only in sample GSM1. The detection of the red lake by PLM and ESEM-EDX due to the high peak of Al [42], was confirmed in superficial layers by previous reflectance spectroscopy measurements [6].

The FTIR-ATR analysis of the pinkish layer of sample GSM2, in addition to the absorbances referable to lead white, detected the bands related to esters of carboxylic acid, free carboxylic acids and lead carboxylates ($\sim 1540\text{--}1503\text{ cm}^{-1}$), indicating the use of an oily binder, which over time reacted with the Pb^{2-} ions of the pigment. Proteinaceous material was detected too according to the band at 1645 and 1540 cm^{-1} , possibly related to egg binder added to vermilion or to the restoration compounds.

According to PLM and ESEM/EDX, the flesh of Saint Sebastian (sample GSM6, Table S2) is composed of a double layer of lead white, vermilion and rare lead tin-yellow particles. The overlapped blood drop consists of red lake [43], lead white, calcium carbonate and powdered glass particles.

In both samples, GSM1 and GSM6, the red layers showed FTIR-ATR spectra in which both stretching of $\text{CH}_2\text{-CH}_3$ groups at ~ 2925 and 2853 cm^{-1} and stretching of carboxylates (COO^-) around 1575 and 1458 cm^{-1} are visible. No signals due to the anthraquinone compounds of the lake were detected, due to both the low concentration of the dye and the co-presence of peaks of other substances (mainly lipids and carboxylates) in the region of interest. Instead, a signal centered at 1036 cm^{-1} was detected. It can be assigned to silicates and hydrated alumina, a component of the lake [51] (Figure 5).

In the *Visitation* altarpiece, stratigraphic observations of flesh hues showed a pinkish painting layer ($60\text{ }\mu\text{m}$) based on lead white, vermilion, finely grounded glass particles (with a minimum size of $10\text{ }\mu\text{m}$), hematite, red lake and dolomite particles (sample SF1: Figure S8a–c, Table S3). FTIR-ATR attested the presence of lead white, esters of carboxylic acid and lead carboxylates indicating the use of an oily binder.

PLM and ESEM-EDX investigations showed that in the shadow of St. Elisabeth's mantle, the underlayer (with an overall thickness of $228\text{ }\mu\text{m}$) consists of two layers of lead white mixed with red lake and colorless powdered glass (sample SF4: Figure S8c–f, Table S3). The overlapped glaze layer (of $85\text{ }\mu\text{m}$) is mainly rich in the red lake and powdered glass particles with their typical jagged edges. EDX analysis revealed Si, Ca, Na, Al, K, Fe and Mn. The FTIR-ATR of the underlayer showed the presence of lead white, esters of carboxylic acid and lead carboxylates denoting the use of an oily binder. In the red glaze layer, FTIR-ATR detected lead white and esters of carboxylic acid.

In the Virgin's brilliant red dress, the underlayer ($55\text{ }\mu\text{m}$) is composed of vermilion, a small amount of lead white and colorless glass particles. The glaze layer ($15\text{ }\mu\text{m}$) consists of red lake, vermilion, rare bone black particles and calcium carbonate according to EDX spectra (sample SF3: Figure S8g–i, Table S3). The FTIR-ATR spectrum of sample SF3 clearly shows peaks referable to lipids ($2927\text{--}2852$, $1731\text{--}1694\text{ cm}^{-1}$) and proteinaceous compounds (~ 3290 and $\sim 1650\text{ cm}^{-1}$). Conversely, sample SF4 showed two pink layers under the transparent red glaze, both containing lead white and small percentages of lake and glass powder particles. The FTIR-ATR analysis attests that the oily binder appears to be largely converted into lead carboxylates.

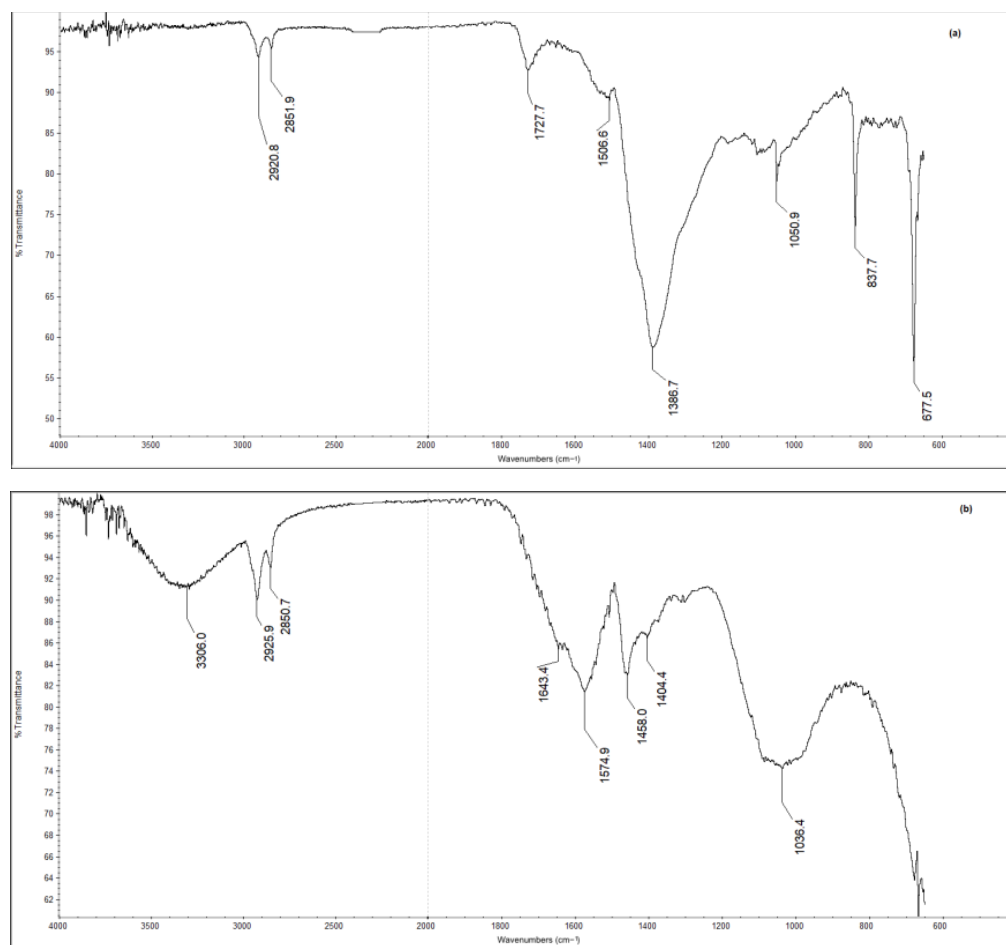


Figure 5. *Martyrdom of Saint Sebastian* panel. FTIR-ATR spectrum of the (a) pinkish and (b) red pictorial layers of sample GSM6.

The red hue of Archangel Raphael's cuff (sample GSS3, Table S4) was obtained with a thick layer (130 μm) based on a red lake with the addition of lead white and powdered glass particles. This layer was then covered with a red lake glaze. The spectrum acquired with FTIR-ATR on the underlayer showed silicates and hydrated alumina related to the red lake, with lead white and calcium oxalate. The presence of the absorptions between 1540 and 1515 cm^{-1} , largely due to carboxylates, suggests the use of oil that reacted with lead white over time, whose absorptions are observed at 1402 and 680 cm^{-1} .

4.5. Binding Media by Means of GC-MS

In GC-MS investigations, the procedure consisted of two main steps: the first one focusing on the lipidic components and the second on the proteinaceous material. Two chromatograms were collected for each sample: the first one from fatty acid derivatives and the second from amino acid derivatives. The GC-MS analysis carried out on the samples of *Visitation* altarpiece (SF1, SF2, SF4), *Martyrdom of Saint Sebastian* panel (GSS7, GSS8) and *Tobias and the Archangel Raphael* canvas (GSM12, GSM13) showed the presence of fatty acids and amino acids. Azelaic (nonanedioic acid, saturated dicarboxylic acid), miristic (C14:0), palmitic (C16:0), oleic (C18:1) and stearic (C18:0) acids were detected (Table S5). In our samples, the value of the azelaic acid/palmitic acid ratio (A/P) is lower than 1 (Table S5) and according to the literature, this value would lead to excluding the presence of any siccativ oil [52]. In an oil and egg mixture, the high palmitic acid content of egg yolk can probably alter the A/P (and also palmitic/stearic) ratio. Furthermore, some scholars mentioned the absence of dicarboxylic acids in oil paintings, as in Santi's samples, probably due to their low methylation recovery in the transesterification reaction [53]. Azelaic acid

is a characteristic marker of aged drying oils produced during the oxidative degradation of fatty acids and the A/P ratio is not constant with time [54,55]. Moreover, the presence of inorganic pigments or organic lacquer could affect the drying process and, as a consequence, the fatty acids profile [56]. Bozan indicated that a low ratio (0.52 and 0.80) between azelaic and palmitic acid (A/P) is the result of the drying process of the lipidic fraction [57].

As the ratio between palmitic and stearic acid (P/S) remains stable over time, it can be considered a useful parameter to obtain information about the type of drying oil used by the artist, i.e., linseed, walnut or poppy seed oils. In fact, values of P/S in the range 1.4–2.1 could refer to linseed oil; 2.4–2.9 to walnut oil and 2.9–4.1 to poppy seed oil [52]. In all the samples, P/S showed values in the range of 1.59–1.75. According to the sub-mentioned statement and being aware that Santi's artworks were subjected to various restoration interventions during the centuries, especially the *Martyrdom of Saint Sebastian* panel and the *Tobias and Archangel Raphael* canvas [5], it was assumed that the low value of azelaic acid may be due both to its partial removal during the conservative history of the paintings and to the repaint intervention containing fresh oil with a low content of azelaic acid. For this reason and due to the results of FTIR analysis, the presence of linseed oil was, however, considered.

The chromatograms related to the proteinaceous material were considered to obtain the quantitative evaluation of the amino acidic profile, obtained after hydrolysis. The GC-MS investigation showed the presence of amino acids in all the samples. The data obtained were evaluated and subjected to PCA. In the PCA score plot (Figure S9), the samples from the *Visitation* altarpiece are aggregated in the positive PC1 quadrant related to the egg standard area. The samples from *Martyrdom of St. Sebastian* (GSS7, GSS8) fitted with animal glue and casein (skimmed milk) standards while the samples from *Tobias and the Archangel Raphael* (GSM12, GSM13) are in the area of the casein reference data [25].

4.6. Colorless Powdered Glass

The occurrence of colorless powdered glass type containing manganese in Santi's painting layers was first suggested by Energy Dispersive X-Ray Fluorescence due to Mn presence, especially in red, pinkish and flesh hues [6].

According to PLM and ESEM/EDX results (Figures 6 and S8, Tables S2–S4), the powdered glass particles were detected in layers containing red lake (in red, flesh and pinkish hues) or verdigris (in green hues).

The glass particles measured up to 30 μm in the painting layers of the *Visitation*, 30 μm in the *Martyrdom of Saint Sebastian* and 45 μm in the *Tobias and the Archangel Raphael*. ESEM/EDX analysis showed an elemental pattern composed of silicon, calcium, sodium, aluminum, magnesium, potassium, iron and manganese, which clearly distinguish the glassy material. Table 1 reports the average value related to different glass particles found in the samples, expressed as weight % oxides. The data could be affected by systematic errors since the analyzed area is not exactly that of the glass particle, but also the surrounding area; for this reason, the larger particles were mainly considered. Moreover, red lake could contain other elements (lead, aluminum, potassium and phosphorus) which could interfere with the results. In fact, the Al content of glass particles can be overestimated in the red lake-based layers, ranging from 1.9 to 5.5% while in the green hue, it is 2%. The weight % oxides of glass powdered particles in Santi's samples (Table 1) indicate the use of common glass [58,59]. The glass particles can be classified as sodic type as they contain Na_2O with an average higher than 10%. Moreover, the average amount of K_2O (2.09%) indicates the possible use of plant ash [58].

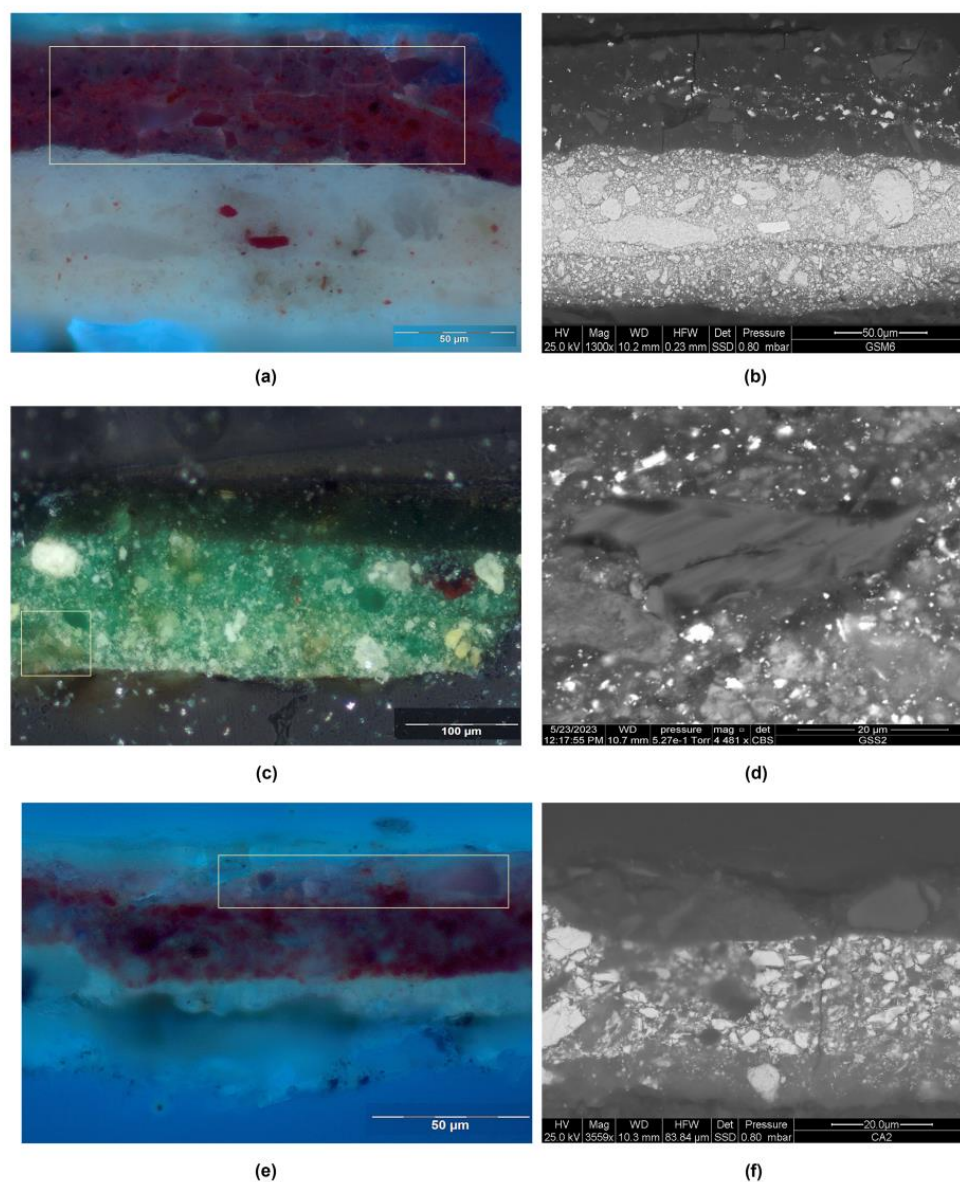


Figure 6. *Martyrdom of Saint Sebastian* panel. Sample GSM6: (a) cross-section, PLM micrograph, UV light, detail of glass particles in the red lake-based glaze layer; (b) ESEM-BSE micrograph, detail of glass particles. Tobias and the Archangel Raphael canvas. Sample GSS1: (c) cross-section, PLM micrograph, visible light; (d) ESEM-BSE micrograph of glass particles found in the underlayer based on green copper acetate. *Communion of the Apostles* panel. Sample CA2: (e) cross-section, PLM micrograph, UV light, detail of glass particles in the red lake-based glaze layer; (f) ESEM-BSE micrograph of glass particle in the glaze layer.

The glass composition (Table 1) related to Giovanni Santi's paintings was compared with that occurred from previous research in the *Communion of the Apostles* panel by Justus of Ghent [11].

Micro-stratigraphic investigations carried out on CA2 and CA7 samples of the *Communion of Apostles* of Justus of Ghent (Table S1) revealed the presence of oil-based priming applied on the gypsum ground layer [10]. The red mantle of the kneeling apostle on the right (sample CA2) consists of an underpaint (40 μm thick) composed of vermilion, lead white, red lake and powdered glass particles with sizes ranging up to 20 μm . The overlayer glaze is composed of red lake and powdered glass particles (Tables S1 and S5, Figure 1c). The Christ's blue robe sample (CA7) is made of a layer (40 μm thick) of ultramarine blue,

lead white, rare grains of red lake, and powdered glass particles measuring up to 20 μm . The glass powdered composition is related to soda lime and Al-poor glass (Table 1).

5. Discussion

The integrated investigations carried out on the *Visitation* altarpiece, the *Martyrdom of Saint Sebastian* panel and *Tobias and the Archangel Raphael* canvas allowed us to improve the knowledge of Giovanni Santi's painting materials and executive technique.

Starting from the wooden supports, Santi used poplar (*Populus* sp.) as attested in other Santi's panel paintings, such as the *Madonna with Child and Two Angels* of the Puskin Museum [60], the *Sacred Conversation* of Montefiorentino and Fano, the *Annunciation*, the Buffi altarpiece and *Christ communicates St. Peter* [1]. This wood species was widely employed in Italy from the late thirteenth to the early fifteenth centuries [61].

Protective layers, composed of gypsum and red lead, were found on the back of both the *Visitation* altarpiece of Fano and the *Martyrdom of St. Sebastian* panel. Dunkerton described the use of the gypsum-based layer on the back of the *Virgin and Child* of the National Gallery [61] and it is also attested in the *Sacred Conversation of Montefiorentino* [6].

While poplar wood supports are common in Santi's wooden artworks, the use of canvas is rare. The painter used a plain weave fabric in *Saint Jerome* (1475–1478) at the Vatican Museums, a herringbone canvas in *Tobias and the Archangel Raphael* and in *Saint Roch* also held in Casa Raffaello, Urbino [2]. Herringbone canvas was very unusual support in Italy at that time and was probably chosen instead of other types of canvas to provide greater consistency to the painting, and perhaps with that experimental attitude that characterizes Santi in certain aspects of his work [6].

The integrated investigations carried out on Santi's paintings indicated the use of one or two ground layers made of gypsum mixed with animal glue applied to receive the paint layers as in the aforementioned *Virgin and Child* panel [62] and in *Tobias and the Archangel Raphael* canvas [2]. In the large panels (*Martyrdom of Saint Sebastian* and *Visitation*), Santi used thick ground layers, whereas in canvas paintings (*Tobias and the Archangel Raphael* and *Saint Roch*), the preparatory layers are thinner, probably to accentuate the texture of the herringbone weave [2].

The presence of anhydrite is often associated with *gesso grosso* [41], due to the partial hydration of burnt gypsum.

In *Tobias and the Archangel Raphael*, a carbon-based ink was detected in the underdrawing, confirming the response obtained by IR reflectographic images [6].

Regarding pigments, micro-invasive analyses confirmed and improved the results obtained through non-invasive investigations carried out on these three paintings in the same areas [6]. The blue hues examined were obtained using finely grounded azurite with few impurities. Hematite particles are probably referable to natural impurities that occurred in azurite [44]. The presence of Ag impurities in azurite could indicate provenance from the silver mines of Saxony, a known source of copper-blue carbonate [63]. Calcium carbonate might be intentionally added as a filler [64], as well as dolomite.

In the green hues, verdigris basic was sometimes used overlapped or mixed with lead-tin yellow (type I), lead white, hematite and rare orpiment particles. The use of verdigris, either pure or mixed with other pigments (lead white, lead-tin yellow), is associated with the oil binder, and powdered glass was found in *Tobias and the Archangel Raphael* painting.

The yellow hues were obtained using lead-tin yellow type I both as an underlayer, combined with green pigments, or in glazes based on Cu-containing pigments (verdigris basic), as usual in that period and later [50]. Yellow ochre was widely detected in yellow and brown colors.

In the red hues, the underlayer is composed of vermilion, lead white and colorless glass particles while the glaze layer is based on red lake and vermilion. Particles of vermilion are always added to brown ochre to reach the deep brown and brown-reddish hues.

In the flesh tones, colorless powdered glass was mixed with lead white, vermilion, bone black, hematite, red lake and dolomite particles, the latter probably intentionally added as a filler or extender, as seen in other mixtures.

According to the FTIR and FTIR-ATR results, as well as the GC-MS data, the presence of oil binders is attested in almost all the samples. Only on the SF samples (*Visitation* altarpiece panel) and on those containing azurite, egg binder was detected. However, we should mention the identification of drying oil in the aged samples using GC/MS is very difficult due to the oxidization/polymerization of the unsaturated fatty acids [56,65] and the conservative history of the artworks has to be considered [5].

The widespread presence of casein and glue in the *Martyrdom of St. Sebastian* and the *Tobias and the Archangel Raphael* could be attributed to the use of these materials in the restoration interventions of the past rather than a voluntary use of them as a binder [66–68]. Past restoration interventions might also be the cause of the frequent occurrence of wax on the *Martyrdom of St. Sebastian* (GSM samples).

The presence of a colorless powdered glass type containing manganese in Santi's painting layers, hypothesized through non-invasive exams [6], was confirmed in the painting layers of the *Visitation*, the *Martyrdom of St. Sebastian* and in *Tobias and the Archangel Raphael*. According to the results, Santi seems to have used this glassy material mainly with the red lake, as it was detected in red glaze layers, as well as in flesh and pink underpaint layers. The addition of powdered glass was also observed in verdigris-based layers, a technical expedient scarcely documented in the literature. Oil binder was attested in all of these painting layers.

The use of glass and nut oils is also attested in Giovanni Santi's *Virgin and Child* of the National Gallery, London, dating from 1488 [62] and in the *Music* painted by Justus of Ghent dated from the 1470s and probably realized in Urbino [58].

The occurrence of colorless powdered glass particles was attested in the latter author's *Communion of Apostles*, not only in the red lake-based layer, but also in a blue pictorial layer: an occurrence that seems quite rare for that time. While the presence of red lake in this blue layer containing natural ultramarine could explain the glass, the minimal number of red lake particles suggest that the glass was not solely due to the red lake and might have been used to maintain layer transparency, thereby taking advantage of the intricate and rich underdrawing [69]. The comparison between the elemental composition of powdered glass particles in Santi's paintings and the *Communion of the Apostles* showed quite similar values, indicating they both used a soda lime Al-poor glass, which aligns with the Italian type rather than the German or Dutch types. This composition is related to the use of river pebbles as a possible source [58]. Starting already from the 14th century, Venetian glassmakers used quartz pebbles instead of silica sand to reduce coloring contaminants such as iron, alongside a Levantine source of flux, soda-lime coastal plant ash [59].

In light of these results, with regard to the glass powdered function, it is likely that the colorless powdered glass was used as a filler to create overlapped translucent layers, without significantly modifying the refractive index of the binder, i.e., giving more body to the layers and providing transparency that other fillers would not have allowed.

Recent studies on the drying properties of the powdered glass in red lake layers showed that they did not produce significant differences in drying time, but they noted that the glass additions made the madder lake easier to grind and paste with the oil medium [70–72].

Regarding the size of powdered glass, in the Santi paintings, they measure up to 45 μm as attested in the Italian artworks ([70] and references therein). In the *Communion of the Apostles*, the glass particles are smaller than 20 μm , a little bit larger than the size of those found in German and Netherlandish paintings.

6. Conclusions

The large altarpieces were prepared with gesso bound in animal glue given in several layers following traditional Italian practice. Occasionally, a thin priming layer with slight pigmentation was detected, likely used to achieve an off-white surface.

Regarding binders, proteic or lipoproteic material and siccative oil were found, the latter well evidenced using FTIR spectroscopy. This technique ascertained the presence of peaks attributable to the egg in blue or blue-violet samples containing azurite of the *Martyrdom of Saint Sebastian* panel (GSM5, GSM 7 and GSM10), indicating that azurite was bonded with tempera, unlike the other pigments and layers examined, which showed the siccative oil bands.

The GC-MS investigation conducted to identify the paint binder showed the presence of fatty acids and amino acids in all the samples. As regards the lipid material content found in all samples examined, the value of the palmitic acid/stearic acid (P/S) ratio was used to identify the type of drying oil, which turned out to be linseed oil. The PCA graph clearly shows the presence of the egg in the *Visitation* altarpiece's samples; in the samples from the *Martyrdom of Saint Sebastian* panel, animal glue and casein were detected; in the samples from *Tobias and the Archangel Raphael* canvas, mainly casein was found. The presence of casein and glue in the investigated samples could be credited to the use of this material in past restoration interventions.

The stratigraphy usually involves light underpaints (from 50 to 90 μm) containing lead white and other pigments covered with thinner and glaze layers, such as in the draperies, cloths and landscape. The examined glaze layers were widely applied with semi-transparent pigment mixtures containing red lakes or verdigris basic.

The colorless powdered glass was found both in the underpainting and glaze layers that were always related to red lakes and in the green copper acetate oil-based glazes. The refractive index of the glass is similar to that of oil (ca. 1.5), enhancing transparency compared to pigment particles. It is probable that Santi added the glass powder to the lakes and verdigris to provide more body to the layers and—at least in the glazes—to improve transparency, in a way that other fillers would not have allowed. Of course, we cannot exclude that glass could help drying; in fact, historical sources have suggested its use for centuries to expedite oil drying (and in some cases to aid in grinding orpiment). If our hypothesis is correct, we cannot exclude that even before introducing the siccative oil binder some painters tried to add glass in tempera-bounded layers to obtain transparent glazes, pointing towards avenues for future research.

Santi used finely grounded glass particles, referable to a soda-lime glass typical for the Italian area, which became more prevalent in Italian paintings after 1500. In fact, the use of glass powder appears to be substantially new to Italian painting practice, documented in the same years in artworks of Perugino around the same period, while it is typically found in coeval or previous Northern European paintings (Flemish, in particular).

Supplementary Materials: The following supporting information can be downloaded at: <https://www.mdpi.com/article/10.3390/app13179739/s1>, Figure S1. (a) Giovanni Santi, *Martyrdom of Saint Sebastian* (1487–1488); (b) Justus of Gent, *Communion of the Apostles* panel (1473–1474). Figure S2. (a) *Martyrdom of Saint Sebastian* panel: sample GSM9, PLM micrograph of poplar (*Populus* sp.), transmitted light; *Visitation* altarpiece: (b) protective layer in the *verso* of the panel: sample SF8, PLM micrograph of the cross-section in visible light; (c) sample SF9, ESEM, micrograph of linen fibers; (d) *Tobias and the Archangel Raphael*: sample GSS5: BSE micrograph of linen fibers. Figure S3. *Martyrdom of Saint Sebastian* panel. Sample GSM1: (a) PLM micrograph of the cross-section, visible light; (b) ESEM-BSE micrograph; (c) EDX spectrum of the ground layer. Figure S4. *Visitation* altarpiece. Sample SF6. (a) PLM micrograph of the cross-section, visible light; (b) ESEM micrograph, detail of the priming layer; (c) EDX spectrum of priming layer. Figure S5. *Visitation altarpiece*: sample SF1, Raman spectrum of a black particle in the underdrawing. Figure S6. *Martyrdom of Saint Sebastian* panel. Sample GSM5: (a) PLM micrograph of the cross-section, visible light; (b) ESEM-BSE micrograph of azurite particle with Ag impurities; (c) EDX spectrum of blue particle. Sample GSM7: (d) PLM micrograph of the cross-section, visible light; (e) EDX spectrum of red particle; *Visitation altarpiece*.

Sample SF6: (f) FTIR-ATR spectrum of blue pictorial layer. Figure S7. *Martyrdom of Saint Sebastian* panel. Sample GSM4: (a) PLM micrograph of the cross-section in visible light, detail of paint layers; (b) Raman spectra of lead-tin yellow type I with main bands of cerussite and hydrocerussite. Figure S8. *Visitation* altarpiece. Sample SF1: (a) PLM micrograph of the cross-section in visible light, detail; (b) ESEM-BSE micrograph, glass particle in painting layer; (c) EDX spectrum of glass particle. Sample SF4: (d) PLM micrograph of the cross-section in visible light, detail of painting underlayer; (e) ESEM-BSE micrograph, detail of glass particles in pinkish underpaint layer; (f) EDX spectrum of glass particle. Sample SF3: (g) PLM micrograph of the cross-section in visible light, detail; (h) ESEM-BSE micrograph, detail of glass particles in red underpaint layer; (i) EDX spectrum of glass particle. Figure S9. PCA score plot of the relative percentage contents of eight amino acids in 43 reference paint samples [25], (where G: animal glue; C: casein; E: egg; GE: animal glue and egg; GC: animal glue and casein; EC: egg and casein), and the painting samples (SF1, SF2, SF4 from *Visitation* altarpiece; GSM12, GSM13 from *Martyrdom of Saint Sebastian*, GSS7, GSS8 from *Tobias and the Archangel Raphael* canvas). Table S1. Description of the micro-samples and the integrated analyses; Table S2. *Martyrdom of Saint Sebastian*—Integrated stratigraphic analyses; Table S3. *Visitation*—stratigraphic analyses of samples; Table S4. *Tobias and the Archangel Raphael*—stratigraphic analyses of samples; Table S5. The relative percentage of the integrated areas respect the analytes detected by GC-MS analysis for the lipidic fraction.

Author Contributions: Conceptualization, M.L.A.; Data curation, M.L.A., G.P., M.C., F.F. and V.M.; Formal analysis, M.L.A., M.C., E.M., V.M., A.C. and G.G.; Funding acquisition, M.L.A.; Investigation, M.L.A., M.C., V.M., A.C., G.G. and C.P.; Methodology, M.L.A. and M.C.; Project administration, M.L.A. and G.P.; Resources, M.L.A.; Supervision, M.L.A., G.P. and M.C.; Validation, M.L.A.; Visualization, M.L.A. and M.C.; Writing—original draft, M.L.A.; Writing—review and editing, M.L.A., G.P., M.C. and V.M. All authors have read and agreed to the published version of the manuscript.

Funding: This research received no external funding.

Institutional Review Board Statement: Not applicable. This study doesn't involve humans or animals.

Informed Consent Statement: Not applicable. This study doesn't involve humans or animals.

Data Availability Statement: Data Availability Statements are not available.

Acknowledgments: Fabio Frezzato actively collaborated on the ATR-FTIR analysis and the drafting of this work, but he died in the final stages: to his great knowledge of materials and painting techniques, as well as his valuable experience as a chemist, this work is dedicated. This research was carried out according to the agreement intervened between the University of Urbino-DISPEA and Galleria delle Marche for *Giovanni Santi's exhibition* (30 November 2018–17 March 2019). Thanks to Valentina Raspugli for her help in carrying out part of the research and to Pietro Baraldi for the micro-Raman analysis. Thanks to Andrea Bernardini, Alessandro Marchi, Maria Rosaria Valazzi, Agnese Vastano, Alessia Andreotti and Ivica Ljubenkovic for their availability; to Dariia Korsunova and Alina Kiseleva for English language editing. Thanks to Benelli Arte for instrumentation accessibility and Fondazione Cassa di Risparmio of Pesaro for their contribution.

Conflicts of Interest: The authors declare no conflict of interest. The funders had no role in the design of the study; in the collection, analyses or interpretation of data; in the writing of the manuscript; or in the decision to publish the results.

References

1. Amadori, M.L.; Poldi, G. La tecnica pittorica di Giovanni Santi. In *Giovanni Santi. "Da poi... Me Dette Alla Mirabil Arte de Pictura"*, Catalogue of the Exhibition (Urbino, Galleria Nazionale Delle Marche Palazzo Ducale, 30 November 2018–17 March 2019); Valazzi, M.R., Ed.; Silvana Editoriale: Cinisello Balsamo, Italy, 2018; pp. 259–277.
2. Poldi, G.; Amadori, M.L.; Mengacci, V. Technical peculiarities in Giovanni Santi's paintings on canvas. *Materia J. Tech. Art Hist.* **2021**, *1*, 28–42.
3. Valazzi, M.R. (Ed.) *Giovanni Santi. "Da poi... Me Dette Alla Mirabil Arte de Pictura"*, Catalogue of the Exhibition (Urbino, Galleria Nazionale Delle Marche Palazzo Ducale, 30 November 2018–17 March 2019); Silvana Editoriale: Cinisello Balsamo, Italy, 2018.
4. Varese, R. *Giovanni Santi*; Nardini Editore: Fiesole, Italy, 1994.

5. Bernardini, A. Martirio di San Sebastiano (cat. entry no. 25). In *Giovanni Santi, "Da poi... Me Dette Alla Mirabil Arte de Pictura", Catalogue of the Exhibition (Urbino, Galleria Nazionale Delle Marche Palazzo Ducale, 30 November 2018–17 March 2019)*; Valazzi, M.R., Ed.; Silvana Editoriale: Cinisello Balsamo, Italy, 2018; pp. 138–140.
6. Amadori, M.L.; Poldi, G.; Germinario, G.; Arduini, J.; Mengacci, V. Spectroscopic and Imaging Analyses on Easel Paintings by Giovanni Santi. *Appl. Sci.* **2023**, *13*, 3581. [[CrossRef](#)]
7. Falcioni, A. I documenti degli archivi urbinati su Giovanni Santi. In *Giovanni Santi, "Da poi... Me Dette Alla Mirabil Arte de Pictura", Catalogue of the Exhibition (Urbino, Galleria Nazionale Delle Marche Palazzo Ducale, 30 November 2018–17 March 2019)*; Valazzi, M.R., Ed.; Silvana Editoriale: Cinisello Balsamo, Italy, 2018; pp. 241–247.
8. Bottacin, F. *Giusto di Gand e la Comunione del Duca di Urbino*; CLEUP: Padova, Italy, 2021; pp. 69–81.
9. Menù, M.; Itié, E.; Ravaud, E.; Eveno, M.; Lambert, E.; Laval, E.; Reiche, I.; Mazzeo, R.; Amadori, M.L.; Bonacini, I.; et al. Examination of the Uomini Illustri: Looking for the Origins of the portraits in the Studiolo of the Ducal Palace of Urbino. Part 1. In *Studying Old Master Paintings: Technology and Practice*; Spring, M., Ed.; Archetype Publications: London, UK, 2011; pp. 37–43.
10. Mazzeo, R.; Menu, M.; Amadori, M.L.; Bonacini, I.; Itié, E.; Eveno, M.; Joseph, E.; Lambert, E.; Laval, E.; Prati, S. Examination of the Uomini Illustri: Looking for the Origins of the portraits in the Studiolo of the Ducal Palace of Urbino. Part 2. In *Studying Old Master Paintings: Technology and Practice*; Spring, M., Ed.; Archetype Publications: London, UK, 2011; pp. 44–51.
11. Amadori, M.L.; Poldi, G. I materiali e la tecnica pittorica della Comunione. In *La Comunione Degli Apostoli di Giusto di Gand*; Bottacin, F., Ed.; CLEUP: Padova, Italy, 2021; pp. 239–249.
12. Lavalleye, J. *Le Palais Ducal d'Urbino, Les Primitifs Flamands, I, Corpus de la Peinture des Anciens Pays-Bas Méridionaux au XVe Siècle*; Centre National de Recherches 'Primitifs Flamands': Brussels, Belgium, 1964; Volume 7, p. 39.
13. Cennini, C. *Il Libro Dell'arte*; Frezzato, F., Ed.; Neri Pozza: Vicenza, Italy, 2003; pp. 129, 134, 166, 173, 194.
14. Tomasi, F. L'opera letteraria di Giovanni Santi. In *Giovanni Santi. "Da poi... Me Dette Alla Mirabil Arte de Pictura", Catalogue of the Exhibition (Urbino, Galleria Nazionale Delle Marche Palazzo Ducale, 30 November 2018–17 March 2019)*; Valazzi, M.R., Ed.; Silvana Editoriale: Cinisello Balsamo, Italy, 2018; pp. 162–165.
15. Dunkerton, J. Modifications to the traditional egg tempera techniques in Fifteenth-century Italy. In *Early Italian Paintings, Techniques and Analysis: Symposium, Limburg Conservation Institute, Maastricht 9–10 October 1996*; Bakkenist, T., Hoppenbrouwers, R., Dubois, H., Eds.; Archetype Publications: London, UK, 1997; pp. 29–34.
16. Dunkerton, J. Nord e Sud: Tecniche pittoriche nella Venezia rinascimentale. In *Il Rinascimento a Venezia e la Pittura del Nord ai Tempi di Bellini, Dürer, Tiziano, Exhibition Catalogue (Venice, Palazzo Grassi, 5 September 1999–9 January 2000)*; Bompiani: Milano, Italy, 1999.
17. Poldi, G.; Villa, G.C.F. "Cuius pictura est intuenda admirationi" Contributo alla comprensione della tecnica di Antonello. In *Antonello da Messina. Catalogo Completo, Exhibition Catalogue (Roma, Scuderie del Quirinale, 18 March–25 June 2006)*; Lucco, M., Ed.; Silvana Editoriale: Cinisello Balsamo, Italy, 2006; pp. 91–113.
18. Gilbert, C.E. The Two Italian Pupils of Rogier van der Weyden: Angelo Macagnino and Zanetto Bugatto. *Arte Lomb. Nuova Ser.* **1998**, *122*, 5–18. Available online: <https://www.jstor.org/stable/43106306> (accessed on 10 December 2022).
19. Averlino, A. *Detto il Filarete, Trattato di Architettura*; Finoli, A.M., Grassi, L., Eds.; Il Polifilo: Milano, Italy, 1972; pp. 265, 668–669.
20. Harding, C. Review of: Giotto to Durer. Early Renaissance Painting in the National Gallery; Dunkerton, J., Foister, S., Gordon, D., Penny, N., Eds. *RACAR Rev. D'art Can. Can. Art Rev.* **1992**, *19*, 147–149. Available online: <http://www.jstor.org/stable/42630507> (accessed on 20 January 2023).
21. Bomford, D.; Dunkerton, J.; Gordon, D.; Roy, A.; Kirby, J. Art in the Making: Italian Painting before 1400. *Stud. Conserv.* **1990**, *35*, 163–165. [[CrossRef](#)]
22. Macchioni, N. Species Identification. In *In Situ Assessment of Structural Timber. RILEM State of the Art Reports*; Kasal, B., Tannert, T., Eds.; Springer: Dordrecht, The Netherlands, 2010; Volume 7, pp. 105–107. [[CrossRef](#)]
23. Cartwright, C.R. The Principles, Procedures and Pitfalls in Identifying Archaeological and Historical Wood Samples. *Ann. Bot.* **2015**, *116*, 1–13. [[CrossRef](#)] [[PubMed](#)]
24. Casoli, A.; Santoro, S. Organic materials in the wall paintings in Pompei: A case study of Insula del Centenario. *Chem. Cent. J.* **2012**, *6*, 107. [[CrossRef](#)]
25. Lanterna, G.; Mairani, A.; Matteini, M.; Rizzi, M.; Vigato, A. Characterisation of Decay Markers on Pictorial Models Simulating Ancient Polychromies: Target 2.2.2 of the Special Project on Cultural Heritage—CNR—Italy. In *Proceedings of the 2nd International Congress on Science and Technology for the Safeguard of Cultural Heritage in the Mediterranean Basin, Paris, France, 5–9 July 1999*; Elsevier: Paris, France, 1999; pp. 487–489.
26. Arbizzani, R.; Casellato, U.; Fiorin, E.; Nodari, L.; Russo, U.; Vigato, P.A. Decay markers for the preventative conservation and maintenance of paintings. *J. Cult. Herit.* **2004**, *5*, 167–182. [[CrossRef](#)]
27. Casoli, A.; Montanari, A.; Palla, G. Painted models simulating ancient polychromies: A statistical analysis of chemical results. In *Proceedings of the 3rd International Congress on Science and Technology for the Safeguard of Cultural Heritage in the Mediterranean Basin, Paris, France, 9–14 July 2001*; Elsevier: Paris, France, 2001; pp. 839–845.
28. El-Gaoudy, H.; Kourkoumelis, N.; Varella, E.; Kovala-Demertzi, D. The effect of thermal aging and color pigments on the Egyptian linen properties evaluated by physicochemical methods. *Appl. Phys. A* **2011**, *105*, 497–507. [[CrossRef](#)]
29. Gettens, R.J.; Mrose, M.E. Calcium Sulphate Minerals in the Grounds of Italian Paintings. *Stud. Conserv.* **1954**, *1*, 174–189. Available online: <https://www.jstor.org/stable/1505020> (accessed on 11 November 2022).

30. Bishop, J.L.; Lane, M.D.; Dyar, M.D.; King, S.J.; Brown, A.J.; Swayze, G.A. Spectral properties of Ca-sulfates: Gypsum, bassanite, and anhydrite. *Am. Miner.* **2014**, *99*, 2105–2115. [[CrossRef](#)]
31. Brooker, M.H.; Sunder, S.; Taylor, P.; Lopata, V.J. Infrared and Raman spectra and R-ray diffraction studies of solid lead (II) carbonates. *Can. J. Chem.* **1983**, *61*, 494–502. [[CrossRef](#)]
32. Meilunas, R.J.; Bentsen, J.G.; Steinberg, A. Analysis of Aged Paint Binders by FTIR Spectroscopy. *Stud. Conserv.* **1990**, *35*, 33–51. [[CrossRef](#)]
33. Yang, H.; Irudayaraj, J.; Paradkar, M.M. Discriminant analysis of edible oils and fats by FTIR, FT-NIR and FT-Raman spectroscopy. *Food Chem.* **2005**, *93*, 25–32. [[CrossRef](#)]
34. Otero, V.; Sanches, D.; Montagner, C.; Vilarigues, M.; Carlyle, L.; Lopes, J.A.; Melo, M.J. Characterization of metal carboxylates by Raman and infrared spectroscopy in works of art. *J. Raman Spectrosc.* **2014**, *45*, 1197–1206. [[CrossRef](#)]
35. White, R.L. Infrared spectroscopic investigations of calcium oxalate monohydrate (whewellite) dehydration/rehydration. *Minerals* **2023**, *13*, 783. [[CrossRef](#)]
36. Dallongeville, S.; Garnier, N.; Rolando, C.; Tokarski, C. Proteins in art, archaeology, and paleontology: From detection to identification. *Chem. Rev.* **2016**, *116*, 2–79. [[CrossRef](#)]
37. Svečnjak, L.; Baranovič, G.; Vincekovič, M.; Prđun, S.; Bubalo, D.; Tlak Gajger, I. An approach for routine analytical detection of beeswax adulteration using FTIR-ATR spectroscopy. *J. Apic. Sci.* **2015**, *59*, 37–49. [[CrossRef](#)]
38. Dunkerton, J.; Spring, M. The development of painting on coloured surfaces in sixteenth-century Italy. *Stud. Conserv.* **1998**, *43*, 120–130. [[CrossRef](#)]
39. Jawhari, T.; Roid, A.; Casado, J. Raman spectroscopic characterization of some commercially available carbon black materials. *Carbon* **1995**, *33*, 1561–1565. [[CrossRef](#)]
40. Bruni, S.; Cariati, F.; Casadio, F.; Toniolo, L. Identification of pigments on a XV century illuminated parchment by Raman and FTIR microspectroscopies. *Spectrochim. Acta A Mol. Biomol. Spectrosc.* **1999**, *55*, 1371–1377. [[CrossRef](#)]
41. Liu, Y.; Wang, A.; Freeman, J.J. Raman, MIR, and NIR spectroscopic study of calcium sulfates: Gypsum, bassanite, and anhydrite. In Proceedings of the 40th Lunar and Planetary Science Conference, The Woodlands, TX, USA, 23–27 March 2009; p. 2128.
42. Kingma, K.; Hemley, J.R. Raman spectroscopic study of microcrystalline silica. *Amer. Mineral.* **1994**, *79*, 269–273.
43. Spring Kirby, J.; Spring, M.; Higgitt, C. The technology of red lake pigment manufacture: Study of the dyestuff substrate. *Natl. Gallery Tech. Bull.* **2005**, *6*, 71–87.
44. Aru, M.; Burgio, L.; Rumsey, M.S. Mineral impurities in azurite pigments: Artistic or natural selection? *J. Raman Spectrosc.* **2014**, *45*, 1013–1018. [[CrossRef](#)]
45. Miliani, C.; Rosi, F.; Daveri, A.; Brunetti, B.G. Reflection infrared spectroscopy for the non-invasive in situ study of artists' pigments. *Appl. Phys. A* **2012**, *106*, 295–307. [[CrossRef](#)]
46. Salvadó, N.; Butí, S.; Aranda, M.A.G.; Pradell, T. New insights on blue pigments used in 15th century paintings by synchrotron radiation-based micro-FTIR and XRD. *Anal. Methods* **2014**, *6*, 3610–3621. [[CrossRef](#)]
47. Salvadó, N.; Butí, S.; Cotte, M.; Cinque, G.; Pradell, T. Shades of green in 15th century paintings: Combined microanalysis of the materials using synchrotron radiation XRD, FTIR and XRF. *Appl. Phys. A* **2013**, *111*, 47–57. [[CrossRef](#)]
48. Price, B.A.; Pretzel, B.; Quillen Lomax, S. (Eds.) *Infrared and Raman Users Group Spectral Database*, 2007th ed.; IRUG: Philadelphia, PA, USA, 2009; Volume 1–2. Available online: www.irug.org (accessed on 20 June 2014).
49. Vagnini, M.; Vivani, R.; Sgamellotti, A.; Miliani, C. Blackening of lead white: Study of model paintings. *J. Raman Spectrosc.* **2020**, *51*, 1118–1126. [[CrossRef](#)]
50. Amadori, M.L.; Poldi, G.; Barcelli, S.; Baraldi, P.; Berzioli, M.; Casoli, A.; Marras, S.; Pojana, G.; Villa, G.C.F. Lorenzo Lotto's painting materials: An integrated diagnostic approach. *Spectrochim. Acta A Mol. Biomol. Spectrosc.* **2016**, *164*, 110–122. [[CrossRef](#)]
51. Retko, K.; Legan, L.; Ropret, P. SERS procedure using photoreduced substrates and reflection FTIR spectroscopy for the study of natural organic colourants. *J. Raman Spectrosc.* **2021**, *52*, 130–144. [[CrossRef](#)]
52. Colombini, M.P.; Modugno, F.; Fuoco, R.; Tognazzi, A. A GC-M Study on the deterioration of lipidic paint binders. *Microchem. J.* **2002**, *73*, 175–185. [[CrossRef](#)]
53. Blaško, J.; Kubinec, R.; Husová, B.; Příklad, P.; Pacáková, V.; Štulík, K.; Hradilová, J. Gas chromatography/mass spectrometry of oils and oil binders in paintings. *J. Sep. Sci.* **2008**, *31*, 1067. [[CrossRef](#)] [[PubMed](#)]
54. Mills, S.; White, R. Analyses of paint media. *Natl. Gal. Tech. Bull.* **1980**, *4*, 65–67.
55. Ion, R.-M.; Iancu, L.; Grigorescu, R.M.; Slamnoiu-Teodorescu, S.; Dulama, I.D.; Bucurica, I.A. Degradation Products Assessment of the Wooden Painted Surfaces from a XVIIth Heritage Monastery. *Appl. Sci.* **2023**, *13*, 2124. [[CrossRef](#)]
56. Wei, S.; Pintus, V.; Pitthard, V.; Schreiner, M.; Guoding Song, G. Analytical characterization of lacquer objects excavated from a Chu tomb in China. *J. Archaeol. Sci.* **2011**, *38*, 2667–2674. [[CrossRef](#)]
57. Bozan, B.; Temelli, F. Chemical composition and oxidative stability of flax, safflower and poppy seed and seed oils. *Bioresour. Technol.* **2008**, *99*, 6354–6359. [[CrossRef](#)] [[PubMed](#)]
58. Spring, M. Colourless Powdered Glass as an Additive in Fifteenth- and Sixteenth-Century European paintings. *Natl. Gallery Tech. Bull.* **2012**, *33*, 4–26.
59. Verità, M.; Biron, I. Analytical Investigation of Genuine Renaissance Venetian Enamelled and Gilded Glass. *J. Glass Stud.* **2021**, *63*, 157–196. Available online: <https://www.jstor.org/stable/48635698> (accessed on 6 February 2023).

60. Mankova, V. Madonna con Bambino e due Angeli. In *Giovanni Santi, "Da poi... Me Dette Alla Mirabil Arte de Pictura"*, Catalogue of the Exhibition (Urbino, Galleria Nazionale Delle Marche Palazzo Ducale, 30 November 2018–17 March 2019); Valazzi, M.R., Ed.; Silvana Editoriale: Cinisello Balsamo, Italy, 2018; pp. 135–136.
61. Uzielli, L. Part Two: History of Panel-Making Techniques. In *The Structural Conservation of Panel Paintings: Proceedings of the Symposium at the J. Paul Getty Museum, Los Angeles, CA, USA, 24–28 April 1995*; Dardes, K., Rothe, A., Eds.; Getty Conservation Institute: Los Angeles, CA, USA, 1998; pp. 109–185.
62. Dunkerton, J. Osservazioni sulla tecnica della Madonna londinese di Giovanni Santi. In *Giovanni Santi: Proceedings of International Symposium, Urbino, Italy, 17–19 Marzo 1995*; Varese, R., Ed.; Electa: Milano, Italy, 1999; pp. 57–60.
63. Anderson, J. *Riches of the Earth: Ornamental, Precious and Semiprecious Stones*; W.H. Smith Publishers: New York, NY, USA, 1981.
64. De Viguerie, L.; Glanville, H.; Ducouret, G.; Jacquemot, P.; Dang, P.A.; Walter, P. Re-interpretation of the Old Masters' practices through optical and rheological investigation: The presence of calcite. *Comptes Rendus Phys.* **2018**, *19*, 543–552. [[CrossRef](#)]
65. Schönemann, A.; Kenndler, E.; Frenzel, W.; Unger, A. An Investigation of the Fatty Acid Composition of New and Aged Tung Oil. *Stud. Conserv.* **2006**, *51*, 99–110. [[CrossRef](#)]
66. Mills, J.; White, R. *Organic Chemistry of Museum Objects*, 2nd ed.; Routledge (Taylor & Francis Group): New York, NY, USA, 1999; pp. 65–66.
67. Beutel, S.; Klein, K.; Knobbe, G.; Konigfeld, P.; Petersen, K.; Ulber, R.; Schelper, T. Controlled enzymatic removal of damaging casein layers on medieval wall paintings. *Biotechnol. Bioeng.* **2002**, *80*, 13–21. [[CrossRef](#)] [[PubMed](#)]
68. Cattò, C.; Gambino, M.; Cappitelli, F.; Duce, C.; Bonaduce, I.; Forlani, F. Sidestepping the challenge of casein quantification in ancient paintings by dot-blot immunoassay. *Microchem. J.* **2017**, *134*, 362–369. [[CrossRef](#)]
69. Poldi, G. Disegno e conservazione nella 'Pala del Corpus Domini', tra Giusto di Gand e Paolo Uccello. In *La Comunione Degli Apostoli di Giusto di Gand*; Bottacin, F., Ed.; CLEUP: Padova, Italy, 2021; pp. 203–238.
70. Lutzenberger, K.; Stege, H.; Tilenschi, C. A note on glass and silica in oil paintings from the 15th to the 17th century. *J. Cult. Herit.* **2010**, *11*, 365–372. [[CrossRef](#)]
71. Almasian, M.; Tiennot, M.; Fiskeand, L.D.; Hermens, E. The use of ground glass in red glazes: Structural 3D imaging and mechanical behaviour using optical coherence tomography and nanoindentation. *Herit. Sci.* **2021**, *9*, 66. [[CrossRef](#)]
72. Cooper, L.; Pierre, A.; Ravaud, E.; Mélinge, Y.; Majérus, O.; Caurant, D.; Bastian, G.; Eveno, M.; Andraud, C.; Tournié, A. Influence of the addition of crushed glass on the physical and chemical properties of lead white oil paint. *J. Cult. Herit.* **2023**, *61*, 238–246. [[CrossRef](#)]

Disclaimer/Publisher's Note: The statements, opinions and data contained in all publications are solely those of the individual author(s) and contributor(s) and not of MDPI and/or the editor(s). MDPI and/or the editor(s) disclaim responsibility for any injury to people or property resulting from any ideas, methods, instructions or products referred to in the content.